Structural and Microtubule Binding Properties of Tau Mutants of Frontotemporal Dementias†

Daniela Fischer,‡ Marco D. Mukrasch,‡ Martin von Bergen,§ Aleksandra Klos-Witkowska,‡,|| Jacek Biernat,§ Christian Griesinger,‡ Eckhard Mandelkow,§ and Markus Zweckstetter*,‡,⊥

Department for NMR-based Structural Biology, Max Planck Institute for Biophysical Chemistry, Am Fassberg 11, 37077 Göttingen, Germany, DFG Research Center for the Molecular Physiology of the Brain (CMPB), Göttingen, Germany, Department of Medical Physics, University of Silesia, Uniwersytecka 4, 40007 Katowice, Poland, and Max Planck Unit for Structural Molecular Biology c/o DESY, Notkestrasse 85, 22607 Hamburg, Germany

Received June 30, 2006; Revised Manuscript Received December 18, 2006

ABSTRACT: Several mutations in the gene encoding the microtubule-associated protein tau are responsible for the formation of neurofibrillary inclusions in frontotemporal dementia with Parkinsonism linked to chromosome 17 (FTDP-17). Here we present the high-resolution characterization of the conformational properties of two FTDP-17 mutants of the four-repeat domain of tau, P301L and ΔK280, and their properties for binding to polyanions and microtubules. Multidimensional NMR spectroscopy shows that the mutations do no lead to a significant increase in the level of β-structure in their monomeric state, even though the mutations strongly promote β-structure during aggregation. However, local structural changes are induced in the second repeat. These changes only weakly affect the binding to the polyanion heparin, which promotes paired helical filament formation. The extent of binding to microtubules, however, is strongly decreased. Our results demonstrate that the reversible binding of tau to microtubules involves specific interactions, which are not essential for binding to polyanions.

Several neurological disorders such as Alzheimer's disease, Parkinson's disease, Pick's disease, and frontotemporal dementia with Parkinsonism linked to chromosome 17 (FTDP-17)[1] are accompanied by the formation of filamentous inclusions in neurons. These consist mainly of the microtubule-associated protein tau (*1*−*7*).

Tau can aggregate into Alzheimer-like paired helical filaments (PHFs) as an intact protein, 352−441 residues in length (depending on isoform), so that all six tau isoforms are found in Alzheimer PHFs (*8*, *9*). The isoforms differ by two inserts near the N-terminal end and the presence of either four or three imperfect repeat sequences in the C-terminal half of the protein (Figure 1). The region comprising the repeat sequences forms the core of PHFs (*10*) and also promotes PHF assembly in vitro (*11*, *12*). For PHF aggregation, two hexapeptides at the beginning of the second and third repeats (275-VQIINK-280 and 306-VQIVYK-311, respectively) are crucial. These are able to initiate the aggregation of tau into bona fide PHFs with their specific β-sheet-based molecular architecture termed cross-β-structure and thereby represent minimal tau−tau interaction motifs (*3*, *13*).

The physiological function of tau is the regulation of MT stability, neurite outgrowth, and other MT-dependent functions. The three or four repeats in the C-terminal half of the protein and the flanking proline-rich basic domains are known to be involved in MT binding (*14*, *15*). The affinity is regulated by phosphorylation particularly at KXGS motifs in the repeats (*16*).

In hereditary FTDP-17, several mutations within the tau gene are known which give rise to neurofibrillary deposits (*2*−*4*, *6*). They include missense mutations (e.g., G272V, N279K, P301L, and R406W), a deletion (ΔK280), a silent mutation (L284L), and intronic mutations which do not change the protein sequence but affect the ratio of three-repeat to four-repeat tau isoforms (*13*, *17*). The missense and deletion mutants are concentrated in the repeat domain of tau (*14*, *18*, *19*). In vitro and in cell culture experiments, some of the mutations weaken the binding of tau to MTs (*20*−*22*), affect the assembly of MTs, and enhance PHF aggregation (*4*). In particular, the mutants P301L and ΔK280 have a much stronger tendency to aggregate (*4*, *23*). Some mutations, including P301L, also make tau more prone to hyperphosphorylation in cells (*24*).

Tau has a hydrophilic character, is highly soluble, and belongs to the class of natively unfolded proteins with no apparent ordered secondary structure that can be detected by far-UV CD or Fourier transform infrared spectroscopy (*3*, *13*, *19*). Because of its high flexibility, it cannot be studied

† This work was supported by the MPG (to E.M. and C.G.), the EU through UPMAN (to M.Z.), the DFG Center for Molecular Physiology of the Brain (CMPB) (to M.Z.), and the DFG through Grant GK 782 to C.G. and through a DFG Emmy Noether Fellowship to M.Z. (ZW 71/1−5). M.M. is the recipient of a Boehringer Ingelheim fellowship.

* To whom correspondence should be addressed. E-mail: mzwecks@gwdg.de. Telephone: ++49 551 201 2220. Fax: ++49 551 201 2202.

‡ Max Planck Institute for Biophysical Chemistry.

§ Max Planck Unit for Structural Molecular Biology c/o DESY.

|| University of Silesia.

⊥ DFG Research Center for the Molecular Physiology of the Brain (CMPB).

[1] Abbreviations: CD, circular dichroism; FTDP-17, frontotemporal dementia with Parkinsonism linked to chromosome 17; HSQC, heteronuclear single-quantum coherence; K18, four-repeat domain of tau; MT, microtubule; PHF, paired helical filament; wt, wild type.

10.1021/bi061318s CCC: $37.00
Published on Web 02/13/2007

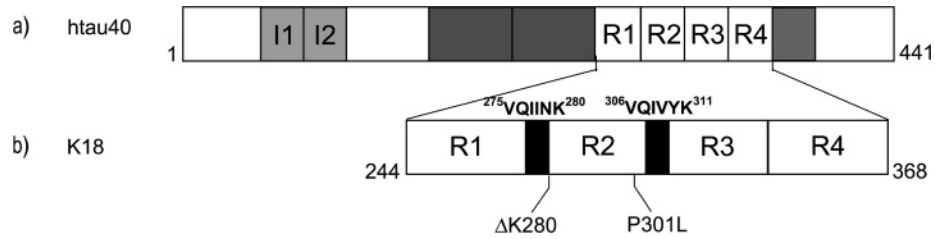

FIGURE 1: Tau isoforms, the repeat domain, and FTDP-17 mutations. (a) htau40 is the largest isoform in the human central nervous system (441 residues). The C-terminal half contains three or four pseudorepeats (~31 residues each, R1−R4). Repeat 2 and the two near-N-terminal inserts (I1 and I2) may be absent due to alternative splicing. Most FTDP-17 mutations are located in the repeat domain. (b) Construct K18 [130 residues, (M)Q244−E372] comprises only the four repeats. The positions of the aggregation-prone hexapeptide motifs 275-VQIINK-280 and 306-VQIVYK-311 in R2 and R3, respectively, are highlighted. The mutations ΔK280 and P301L lie near the hexapeptide motifs and increase their tendency to aggregate. The numbering of residues follows that of the longest isoform.

by high-resolution X-ray crystallography. X-ray analyses exist only in the form of solution scattering and fiber diffraction. Recently, we and others have shown that the repeat domain of tau contains regions of residual β-structure, which have the potential to serve as seeds for aggregation of tau into PHFs (*25*, *26*). The same regions were involved in binding to MTs and polyanions (*25*), supporting the hypothesis that stable MTs prevent PHF formation by blocking the tau−polyanion interaction sites, which are crucial for paired helical filament formation (*11*, *27*).

Here we report the high-resolution characterization of the conformational properties of two FTDP-17 mutants of the four-repeat domain of tau (K18), P301L and ΔK280, and their properties for binding to the polyanion heparin and to MTs. The mutations do not change the secondary structure propensity of the repeat domain of tau, even though they strongly promote β-structure during aggregation. However, the mutations induce conformational changes in repeat 2 and strongly attenuate the binding to microtubules, whereas the interaction with heparin is only slightly affected.

MATERIALS AND METHODS

Expression of Recombinant Tau Constructs and Isotope Labeling. P301L and ΔK280 mutations in the K18 construct (residues Q244−E372 of the longest tau isoform in the human brain plus an initial M243, 130 residues) were created by site-directed mutagenesis using the Quick-change kit (Stratagene, Amsterdam, The Netherlands). The introduced modifications were verified by DNA sequencing. Expression, purification, and isotope labeling were performed as described previously (*25*). NMR samples contained 0.9−1.5 mM ^{15}N-labeled or ^{15}N- and ^{13}C-labeled protein in 95% H_2O/5% D_2O, 50 mM phosphate buffer (pH 6.8) with 1 mM dithiothreitol.

Preparation of MTs. Porcine brain tubulin was purified as described previously (*14*) and incubated at concentrations higher than 200 μM in MT assembly buffer [100 mM Pipes (pH 6.9), 1 mM EGTA, 1 mM $MgSO_4$, and 1 mM DTT] in the presence of 1 mM GTP at 37 °C for 5 min. After the addition of 100 μM paclitaxel (Sigma-Aldrich Chemie, Munich, Germany), polymerization was performed for 20 min at 37 °C.

CD Spectroscopy. All measurements were carried out with a Jasco J-715 CD spectrometer (Jasco, Gross-Umstadt, Germany) in a cuvette with a path length of 0.1 cm. The spectra were recorded between 190 and 240 nm at a scanning speed of 100 nm/min, a bandwidth of 1.0 nm, and a response time of 0.5 s. In each experiment, three spectra were summed and averaged. For calculation of the mean residue ellipticity, the protein concentration was obtained by using the second channel of the CD spectrometer and measuring the absorption of the protein sample at 214 nm (where absorption is dominated by the peptide bonds). Calibration at 214 nm was done with a BSA standard.

NMR Spectroscopy. NMR spectra were acquired at 5 °C on Bruker DRX 800, Avance 700, Avance 600, and DRX 600 spectrometers. Aggregation did not occur at 5 °C in the absence of polyanions. NMR data were processed and analyzed using nmrPipe (*28*) and Sparky 3 (www.cgl.ucsf.edu/home/sparky/). Three-dimensional triple-resonance experiments were conducted to obtain sequence-specific assignments for the backbone of K18P301L and K18ΔK280. Secondary chemical shifts were calculated using NMRView (*29*) as the difference between the measured Cα and C′ chemical shifts and the empirical, sequence-corrected random coil values (*30*, *31*) for the appropriate amino acid type at pH 2.3. Random coil values for the pH sensitive residues histidine, glutamate, and aspartate were taken from Wishart et al. (*32*) for a better accordance of the pH value and our experimental conditions. Random coil values for residues preceding Pro were taken from Wishart et al. (*33*). The averaged value for Cα and C′ was defined as $\Delta\delta_{av}(C\alpha C') = (3\Delta C\alpha + 4\Delta C')/7$. To clarify the effect of the chosen random coil values, we also calculated the secondary Cα chemical shifts using for all amino acid types the random coil values as determined by Wishart et al. (*33*).

Tau−heparin titrations were carried out at pH 6.8 using uniformly ^{15}N- and ^{13}C-labeled protein containing 150 μM K18P301L in MT assembly buffer and K18ΔK280 in 50 mM phosphate buffer. Heparin (average molecular weight of 3350, 5.8 disaccharide subunits, charge per subunit of −2.5, −0.31 z/Å) was purchased from Sigma. The formation of the tau−heparin complex was tracked by two-dimensional ^{1}H−^{15}N heteronuclear single-quantum coherence (HSQC) spectra for increasing heparin concentrations: 0.015, 0.074, 0.146, 0.284, and 1.17 mM for K18P301L and 0.015, 0.029, 0.071, 0.271, and 1.13 mM for K18ΔK280. For tau−MT titrations, the samples contained 150 μM uniformly ^{15}N- and ^{13}C-labeled K18P301L and K18ΔK280, respectively, in MT assembly buffer. Complex formation was monitored at 5 °C for MT concentrations ($\alpha\beta$-tubulin dimers) of 10.5, 42.0, and 58.0 μM for K18P301L and 42.0, 84.0, and 122.0 μM for K18ΔK280. NaCl was added to one K18ΔK280/MT sample (tau:MT ratio of 5) to yield final concentrations of 150 and 300 mM, respectively. Again, ^{1}H−^{15}N HSQC spectra were recorded at 5 °C. Normalized weighted average chemical

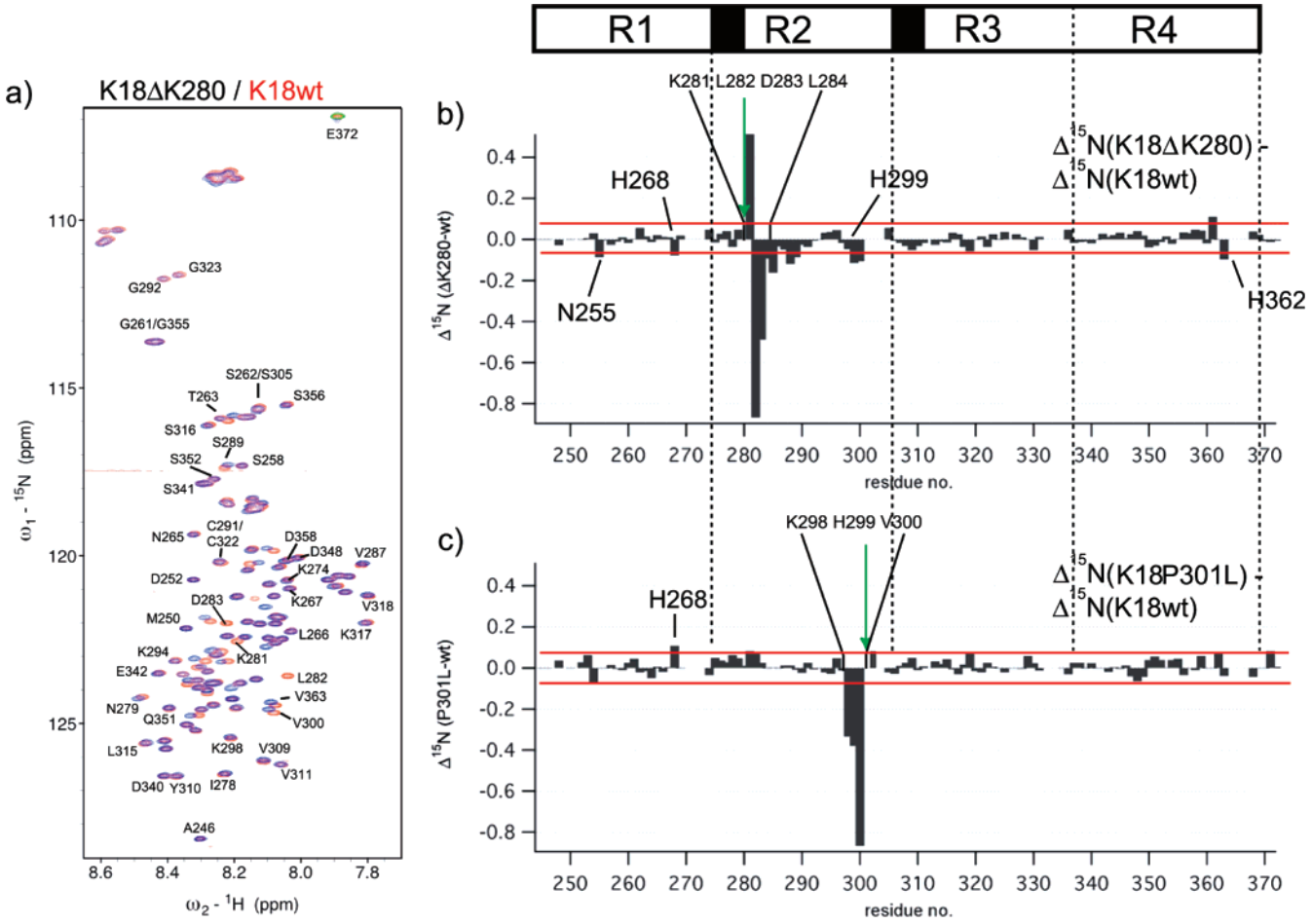

FIGURE 2: Changes in the chemical environment induced by FTDP-17 mutations. (a) Overlay of HSQC spectra for K18ΔK280 (blue) and K18wt (red). Selected sequence-specific assignments are marked. (b) Differences in ^{15}N chemical shifts between K18ΔK280 and K18wt extracted from panel a. (c) Differences in ^{15}N chemical shifts between K18P301L and K18wt. Horizontal lines indicate the average variation of chemical shifts observed for K18wt from sample to sample due to slightly different buffer conditions. Shift changes that exceed the red lines are regarded as significant and are located downstream of ΔK280 and upstream of P301L. Gaps are due to unassigned residues.

shift differences for amide ^{1}H and ^{15}N chemical shifts upon heparin or MT binding were calculated using the equation $\Delta\delta_{av}(NH) = [\Delta H^2 + (\Delta N/5)^2]^{1/2}$, in which ΔH and ΔN are the difference between chemical shifts of the free and bound form.

The aggregation behavior of K18ΔK280 was investigated during a measurement period of 3 days at 5 °C. The signal intensity was monitored by the integration of signals of ^{1}H−^{15}N HSQC spectra, and the relaxation behavior was probed with $T_{1\rho}$ relaxation time measurements. Neither a loss of the monomeric species, detectable via a decreased signal intensity, nor an increase in the level of the oligomeric species, causing a change in the relaxation, was identified. Aggregation, therefore, does not take place under the experimental conditions used here (at 5 °C without polyanions and without agitation).

RESULTS

Backbone Resonance Assignment of K18P301L and K18ΔK280. The ^{1}H−^{15}N HSQC spectra of construct K18, equivalent to the four microtubule binding repeats of full-length tau (Figure 1), and the spectra of both mutants exhibited sharp resonances with a congestion of signals due to the protein's unfolded nature (Figure 2a) (*34*). Starting from the assignment of wild-type (wt) K18, which was previously determined by us (*25*), we were able to assign the mutant proteins by three-dimensional HNCO and high-resolution (HA)CANNH spectra. The sequence PGGG motifs could not be assigned unambiguously due to a strong signal overlap in the glycine region similar to the assignment of the wt protein (this accounts for the gaps in panels b and c of Figure 2 and following). The degeneracy of the glycines in the ^{301}PGGG^{304} motif was partially lifted by the P301L mutation, enabling unambiguous assignment of Leu301 and Gly302. However, the effect of the mutation on Gly303 and Gly304 was not sufficient to resolve the assignment degeneracy of these residues, in agreement with the fact that the mutation primarily influences the upstream residues (see below). For all other residues of K18ΔK280 and K18P301L, the ^{1}H, ^{15}N, ^{13}Cα, and ^{13}C′ chemical shifts were assigned. Changes in the ^{15}N and ^{1}H chemical shifts are pronounced in the vicinity of the mutations, i.e., at residues 281−284 (in C-terminal direction) in the case of K18ΔK280 (Figure 2b) and at residues 298−300 (in the N-terminal direction) in the case of K18P301L (Figure 2c).

Residual Secondary Structure. NMR chemical shifts of Cα and C′ atoms are sensitive indicators of secondary structure in both globular and unfolded proteins (*35*). These shifts show small but distinct deviations from random coil values. The deviations, called secondary chemical shifts, are

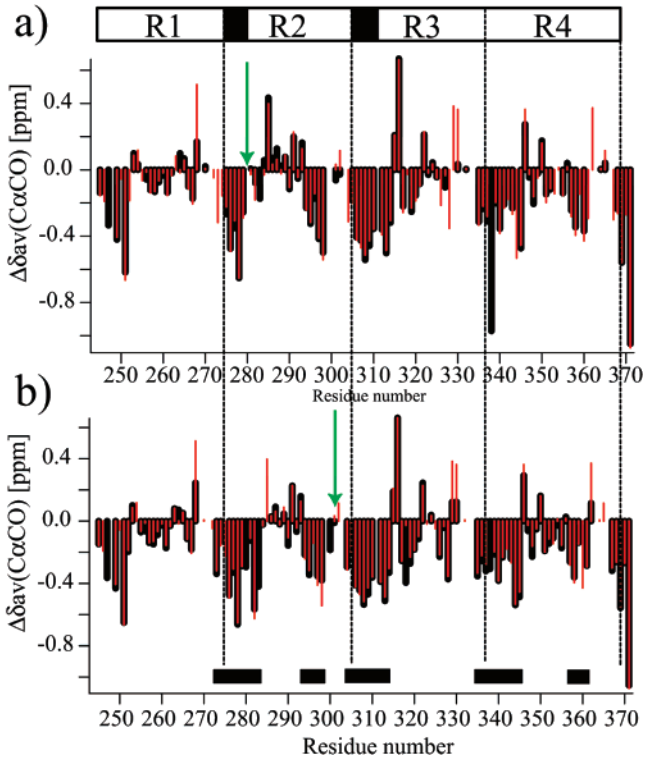

FIGURE 3: Secondary structure propensity of K18ΔK280 and K18P301L. Averaged secondary chemical shifts, $\Delta\delta_{av}$, in K18ΔK280 (a) and K18P301L (b) in comparison to those of K18wt (red bars) at 5 °C in 50 mM phosphate buffer (pH 6.9). The averaged shifts were calculated as $[3\Delta\delta(C\alpha) + 4\Delta\delta(C')]/7$. Five regions of enhanced β-structure propensity (residues 274−284, 295−298, 305−315, 336−345, and 357−361) are indicated by black boxes. They are characterized by contiguous blocks of negative secondary chemical shifts. Residues 246−253 most likely do not have an enhanced β-structure propensity due to the presence of three prolines (P247, P249, and P251). The positions of the mutations are denoted with arrows. All glycines at positions 2 and 3 in the PGGG motifs exhibited identical secondary chemical shifts.

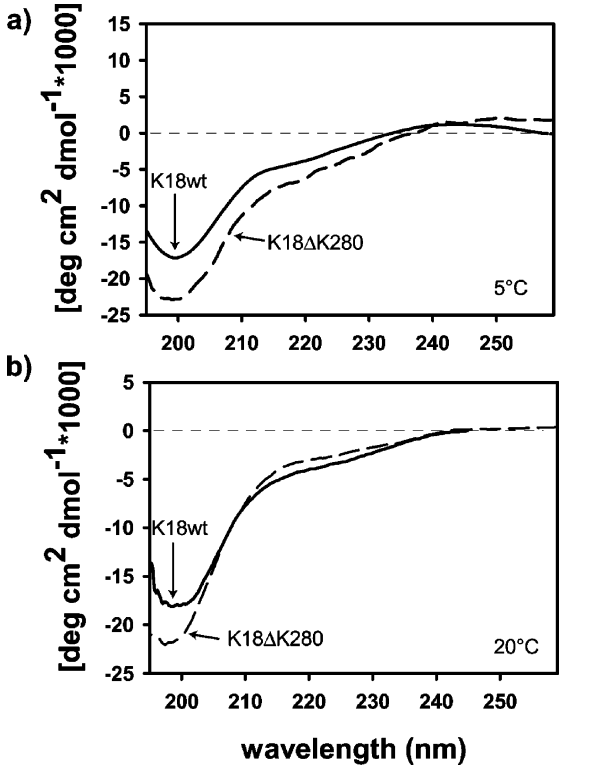

FIGURE 4: Circular dichroism of K18wt and K18ΔK280. The secondary structure content of K18wt (—) and K18ΔK280 (− − −) was measured at 5 (a) and 20 °C (b). The molecular ellipticity was plotted vs the wavelength.

shown in Figure 3. For both mutant proteins, continuous stretches of negative secondary chemical shifts were found for residues 274−284, 295−298, 305−315, 336−345, and 357−361, indicative of a propensity to form β-structure. These stretches encompass the VQIINK and VQIVYK hexapeptide motifs at the beginning of the second and the third repeat, known to be important for the abnormal aggregation of tau into paired helical filaments (PHFs) (*13*). The secondary chemical shifts of the mutants are nearly identical to those in the wild-type protein (Figure 3). The strongest deviations from K18wt were found for histidine residues, most likely due to slight changes in the buffer conditions (the experimental pH is close to the pK_a value of histidines).

The secondary chemical shifts shown in Figure 3 were calculated on the basis of sequence-corrected random coil chemical shifts obtained for G-G-X-G-G peptides (*31*). For comparison, the ΔCα secondary chemical shifts for K18ΔK280 were also calculated using non-sequence-corrected random coil values obtained for G-G-X-A-G-G peptides (*33*). The resulting Cα secondary chemical shift pattern indicated β-structure propensity for the two hexapeptides in the beginning of repeats 2 and 3, similar to what is seen in Figure 2. However, due to the non-sequence-corrected random coil values, the Cα secondary chemical shifts were shifted ∼0.36 ppm toward more positive values (except Asp, Glu, and Cys) such that several continuous stretches of positive secondary chemical shifts appeared. These stretches were previously interpreted as an indication that most of K19 (the construct comprising only three repeats) preferentially populates helical conformations (*26*). Currently, which of the two sets of Cα random coil values is more appropriate cannot unambiguously be determined. However, secondary chemical shift patterns obtained separately for Cα and C′ were more consistent, when the sequence-corrected random coil values were used (as is done here). In addition, no helical propensities were detected for monomeric K18 or K19 by CD and FTIR spectroscopy (*3*) (also see below).

Since the K18ΔK280 and K18P301L mutants have a stronger tendency to aggregate, we considered the possibility of a stronger tendency of the monomer to form β-structure. We therefore used CD spectroscopy to check the conditions of the NMR experiments at different temperatures, because earlier experiments were performed at room temperature, whereas the NMR experiments were performed at 5 °C. The CD spectra show for both K18wt (solid lines) and K18ΔK280 a clear minimum at 200 nm at both 5 and 20 °C (Figure 4; note that the slight differences in the spectra are within the error of the method). The minimum at 200 nm indicates a mostly random coil structure (*36*), and in these monomeric fractions, no increase in the level of β-sheet structure in K18ΔK280 could be observed by CD.

Characterization of the Complexes between Tau Mutants and Polyanions. Polyanions such as heparin are often used to accelerate the assembly of tau into PHFs (*37*−*39*). To observe the formation of a complex between tau and polyanions, the shifts of the backbone amide protons can be

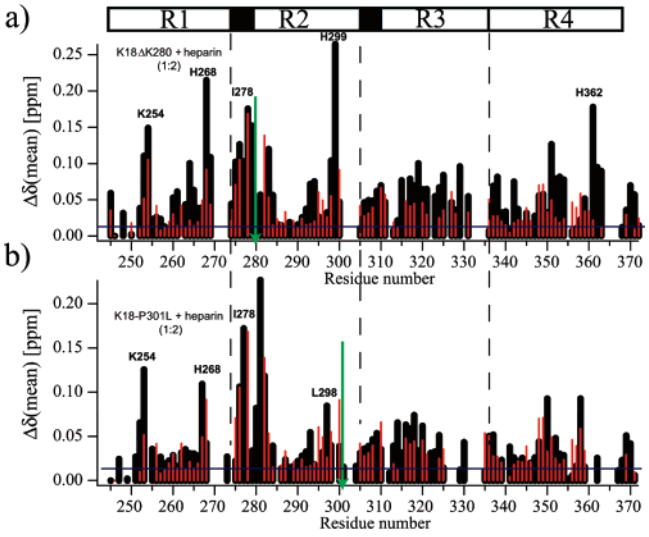

FIGURE 5: Binding of tau mutants to the polyanion heparin. Mean weighted $^1H-^{15}N$ chemical shift changes, $\Delta\delta$(mean), induced by binding of heparin to K18ΔK280 (a) and K18P301L (b) and in comparison to those of K18wt (red bars). The concentration of the tau constructs was 150 μM, and the tau:heparin molar ratio was ~1:2 for K18P301L and K18ΔK280 and ~1:1.5 for K18wt. Horizontal lines indicate the average variation of chemical shifts observed between different samples all containing K18 and heparin (4:1) due to slightly different buffer conditions. Arrows mark the mutation sites. Gaps are due to overlap or the presence of prolines.

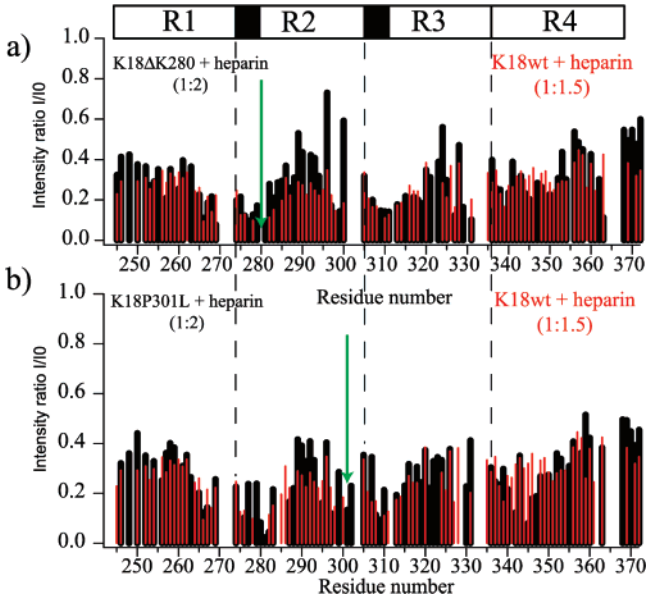

FIGURE 6: $^1H-^{15}N$ signal intensity changes upon addition of heparin. (a) Binding of heparin to K18ΔK280. (b) Binding of heparin to K18P301L. The intensity ratio is calculated as the signal intensity I for a sample with heparin divided by the signal intensity I_0 for a sample without heparin. The tau concentration was 150 μM, and the tau:heparin ratio was ~1:2 for K18P301L and K18ΔK280 and ~1:1.5 for K18wt. For comparison, data for K18wt are also shown (red bars). Arrows mark the mutation sites. Global intensity changes due to partial aggregation are accompanied by intensity reductions in certain regions (V275−L282 and V306−T319), which are caused by a chemical exchange intermediate on the NMR time scale and report on the binding of polyanions to tau.

followed, providing information about the interacting regions and strength of binding. The binding of heparin was monitored by $^1H-^{15}N$ HSQC spectra. This allows one to identify the residues which are important for the binding to polyanions. At higher polyanion concentrations, the change in chemical shift can be accompanied by a decrease in signal intensity, indicating a chemical shift exchange intermediate on the NMR time scale.

For both mutants, large chemical shift changes were present for residues V275−L284, the hexapeptide motif at the beginning of repeat 2 (black bars in Figure 5). In addition, the chemical shifts of selected lysine and histidine residues (L253-K254, H268-N269, L298-H299, and H362) were strongly affected by the addition of heparin. Overall, the patterns of chemical shift changes induced in the mutant proteins were similar to those previously observed for K18wt (red bars in Figure 5). The magnitudes of chemical shift changes at K18mutant-to-heparin ratios of 1:2 were comparable to those measured for a K18wt:heparin ratio of 1:1.5.

In the presence of heparin, K18ΔK280 and K18P301L gradually begin to aggregate like K18wt, as evidenced by a decrease in the overall signal intensity in the $^1H-^{15}N$ HSQC spectra (Figure 6). Besides this overall decrease in signal intensity, resonances of some residues were further broadened by a chemical exchange intermediate on the NMR time scale. In particular, residues in the two hexapeptide motifs (V275−L282 and V306−T319) were attenuated, consistent with their involvement in the binding process. In comparison to those of the wild-type protein, however, the signal intensities of residues S289−S293 appeared to be enhanced, in particular, for K18ΔK280, suggesting a reduced contribution from chemical exchange. The weakened influence of chemical exchange for residues S289−S293 together with the overall slightly lower magnitude of chemical shift changes for the mutant proteins may be interpreted as a reduced affinity for heparin caused by the mutations, potentially due to a less efficient binding of heparin to repeat 2.

Binding of the Repeat Domain of Tau to Microtubules. The binding of K18ΔK280 and K18P301L to MTs was characterized using the NMR chemical shift perturbation method (*40*), in which $^1H-^{15}N$ HSQC spectra were recorded in the presence of increasing amounts of paclitaxel-stabilized MTs. Previous experiments, including sedimentation, SDS−PAGE, and electron microscopy, with the K18 and K19 wild-type protein had already shown that MTs in the paclitaxel-stabilized form are stable at a low temperature (5 °C) during the time course of the NMR measurements (*25*). In general, the shifts observed for the mutants were much weaker than those detected for K18wt (panels a and c of Figure 7). In particular, for K18P301L, only very small chemical shift changes were observed (Figure 7c). In the case of K18ΔK280 and similar to the wt protein, the most strongly shifting residues were histidines and the corresponding hot spot regions, K267-H268, H299-V300, and H329, and in addition E264 (Figure 7a). On the other hand, the resonance positions of residues L253−L256 and V275−L284 stayed almost unchanged upon addition of MTs in clear contrast to those of the wt protein (Figure 7a).

Tau binds to MTs in a biphasic manner. After a first tight and specific binding phase at low tau concentrations, a weak and unspecific binding takes place, resulting in an accumulation of tau on the MT surface (*23*). From a NMR perspective, tau in the MT-bound state is invisible due to the very fast relaxation of the NMR signals. Accordingly, the signal-to-noise ratio in the $^1H-^{15}N$ HSQC spectra decreased rapidly

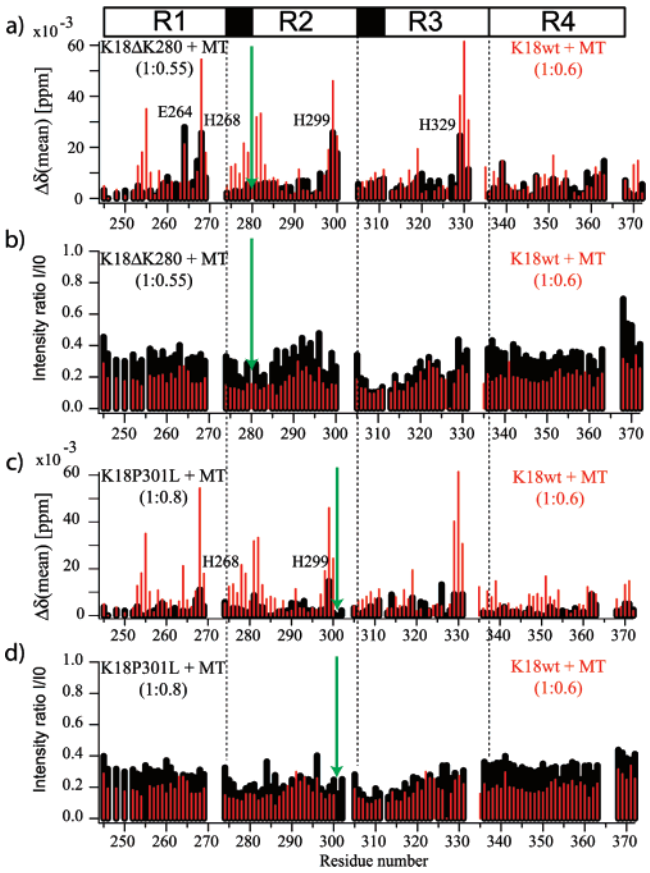

FIGURE 7: Identification of microtubule-binding hot spots in FTDP-17 mutations carrying tau. Mean weighted $^1H-^{15}N$ chemical shift changes of K18ΔK280 (a) and K18P301L (c) and signal intensity ratios in K18ΔK280 (b) and K18P301L (d) between the $^1H-^{15}N$ HSQC spectra of free tau (I_0) and tau in the presence of MTs (I) at 5 °C. Values for K18wt are shown as red bars; arrows mark the mutation sites, and gaps are due to overlap or the presence of prolines. The tau:MT ratio was 1:0.55 for K18ΔK280, 1:0.80 for K18P301L, and 1:0.60 for K18wt. Binding sites were identified on the basis of large chemical shift changes and local intensity reductions due to chemical exchange. Previous experiments with K18 wild-type protein had already shown that MTs in the paclitaxel-stabilized form are stable at a low temperature (5 °C) during the time course of the NMR measurements (*25*).

at higher MT concentrations. Comparison with the wild-type construct (red bars in panels b and d of Figure 7) shows that the intensity decrease is less pronounced for the mutant proteins, with K18ΔK280 even less affected than K18P301L. Despite the smaller reduction in overall signal intensity, however, resonances of residues V306−T319 exhibited a strong attenuation similar to what had been observed for K18wt. The signal intensity in this region is a factor of ∼1.5−2 lower than the average signal intensity for all residues of K18. In summary, chemical shift changes and average signal intensities indicate that the MT binding contribution of the hexapeptide motif in the beginning of repeat 2 was strongly reduced by the ΔK280 mutation, whereas no effect of either the ΔK280 or P301L mutation on the hexapeptide in the beginning of repeat 3 could be detected.

Effect of NaCl on the Binding Affinity for Microtubules. To remove weak unspecific binding and weaken the strong specific binding of tau to MTs so that it can be observed by NMR, NaCl was added in two steps (final concentrations of 150 and 300 mM, respectively) to a sample with a K18ΔK280:

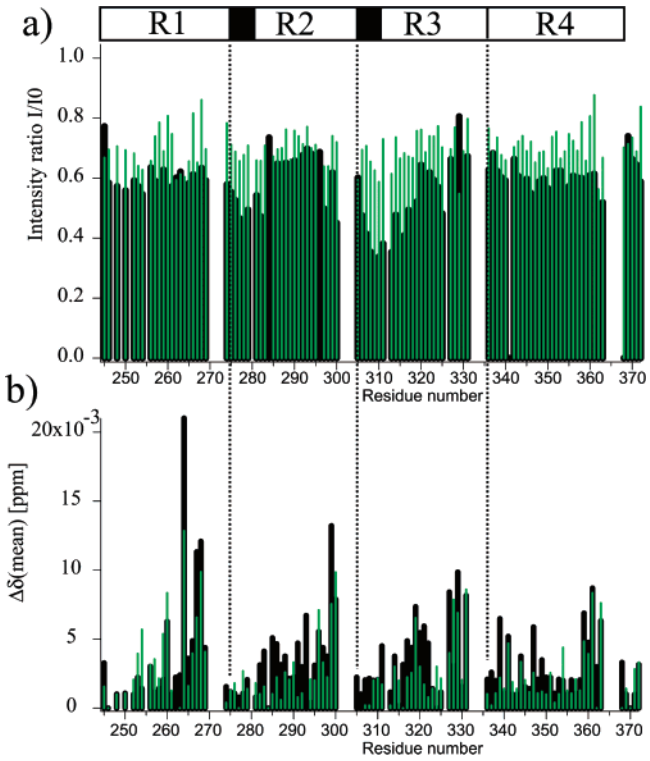

FIGURE 8: Influence of ionic strength on the interaction of K18ΔK280 with preassembled microtubules. Signal intensity ratios (a) and mean weighted $^1H-^{15}N$ chemical shift changes (b) between the $^1H-^{15}N$ HSQC spectra of free tau and tau in the presence of MTs without NaCl (black bars) and with 150 mM NaCl (green bars) (both at 5 °C). The tau:MT ratio was 5:1. For all signal intensity ratio calculations, the reference signal intensity I_0 was obtained from a sample containing K18K280 and the appropriate amount of NaCl, but no MTs.

MT ratio of 5:1 (absolute concentration of tau of 150 μM). At 150 mM NaCl, the overall signal intensity was increased to an average value of 0.71 (Figure 8a). Moreover, the signal intensity was quite uniform across all residues of K18ΔK280. Especially the region around the two hexapeptide motifs, residues K274−L284 and V306−T319, showed a pronounced regain of signal intensity. The regain in NMR signal intensity demonstrates that at 150 mM NaCl the binding of K18ΔK280 to MTs is weakened and many more K18ΔK280 molecules contribute to the observable NMR signal. Nevertheless, strong chemical shift changes were induced by the presence of MTs (green bars in Figure 8b). The strongest shifting residues were residues 260, 264, 267, 268, 299, 329−331, 360, and 361, although the magnitude of these chemical shift changes was reduced in the presence of NaCl. In addition, significantly smaller chemical shift changes were observed for residues 283−289 and 316−323 when the MT titration was performed at 150 mM instead of 0 mM NaCl. This indicates that electrostatic interactions play an important role in binding of K18 to MTs. Importantly, however, the chemical shift changes induced by addition of MTs in the absence of NaCl (when a significant fraction of tau molecules strongly binds to MTs and is therefore invisible to liquid-state NMR spectroscopy) and those at 150 mM NaCl (when most K18ΔK280 molecules contribute to the NMR signal) identify the same regions as being important for MT binding.

DISCUSSION

Tau is one of the major microtubule-associated proteins in the brain. It occurs predominantly in the axons of neurons and promotes the assembly and stability of microtubules. Pathological tau aggregation in the form of filaments, on the other hand, represents one of the hallmarks of a variety of dementias called tauopathies, including Alzheimer's disease, Pick's disease, and FTDP-17. From a biophysial view, tau is an interesting research object as it belongs to the class of "intrinsically disordered" proteins, which can perform a specific function despite the lack of a well-defined three-dimensional structure. Here we have characterized the secondary structure propensity and the properties for binding to polyanions and microtubules of the repeat region of tau (K18), when it carries two mutations that cosegregate with inherited FTDP-17. Knowing the molecular mechanisms that underlie the reduced binding affinity of the ΔK280 and P301L mutants for MTs and for their increased propensity to aggregate might help us to understand the progression of dementia in FTDP-17 patients. Multidimensional NMR spectroscopy is one of the few methods that allow investigation of dynamic proteins such as tau at high resolution.

The major results can be summarized as follows. (1) Both mutations do not significantly influence the secondary structure propensity of K18 in its monomeric state in solution. However, they induce local structural changes in the second repeat. (2) The interaction with the polyanion heparin is slightly weakened by the FTDP-17-associated mutations. (3) The mutations significantly attenuate the binding to microtubules. The more pronounced effect of the mutations on binding to microtubules indicates that the interaction of the repeat domain of tau with microtubules is more specific than the binding to polyanions.

Mutations Induce Local Structural Changes in Repeat 2. NMR chemical shifts of backbone resonances allow a sensitive detection of structural changes, as induced for example by binding of a ligand or by mutations. Even changes in ^{1}H and ^{15}N chemical shifts, which are readily available from two-dimensional correlation spectra, are valuable reporters with respect to the extent of changes induced by mutations. In particular, changes that affect only the immediate vicinity of the site of mutation can be distinguished from those having more global effects. The FTDP-17 mutations ΔK280 and P301L induce the largest changes in the ^{1}H and ^{15}N chemical shifts in repeat 2, i.e., for K18P301L upstream of the mutation site (K298−V300) and for K18ΔK280 downstream (K281−S285). The directionality of the chemical changes caused by the P301L mutation is in agreement with the proposal that the PGGG motif which normally adopts a turn structure is straightened into a more extended structure which includes even the preceding residues K298−V300 (*3*). K18ΔK280, on the other hand, is at the center of a region that preferentially populates β-structure in K18wt. Therefore, the pronounced effect on the upstream residues is not clear.

NMR chemical shifts of backbone atoms, such as Cα and CO, are strongly influenced by secondary structure. In particular, the comparison of secondary chemical shifts in two different states, for example, free and bound to a ligand or wild-type and mutant protein, enables the detection of even small changes in secondary structure propensity. The secondary chemical shifts of K18ΔK280 and K18P301L were highly similar to values observed for K18wt. No strong increase in the propensity to form secondary structure (β or α) was observed for the mutants in solution.

Previous studies had revealed that peptides derived from the repeat domain and containing the K18ΔK280 or P301L mutations had a stronger tendency to aggregate with formation of β-structure, as judged by FTIR and CD (*3*, *4*). However, when the protein was freshly prepared by gel filtration, the monomeric fraction did not exhibit a different content of β-structure (Figure 4). This suggests that the higher rate of aggregation of the two K18 mutants in vitro is not due to an increased content of β-structure in their monomeric, soluble state. Rather, intermolecular interactions become more favorable. The ΔK280 deletion mutation results in a pattern of alternating polar and nonpolar residues, which favors aggregation (*3*, *41*). The P301L missense mutation removes a proline residue from the core of the repeat domain, enabling longer β-strands and a better stacking between strands within the fibril (*3*).

We mention in this context that a predominantly α-helical content has been reported for certain FTDP-17 mutants of tau (*42*). We have not been able to confirm this in experiments using CD and FTIR spectroscopy (*3*, *43*), in agreement with other investigators who have shown that tau has a mostly random coil conformation in solution (*44*−*47*). The discrepancy could possibly be explained by the fact that Jicha et al. (*42*) used tau proteins expressed with polyhistidine tags.

ΔK280 and P301L Mutations Only Weakly Affect the Interaction of K18 with Heparin. It is not clear at present how PHF aggregation is initiated in neuronal cells. However, the fact that in vitro, heparin can greatly improve the polymerizability of tau (*38*, *39*) points to a possible role of cytosolic polyanions [examples are RNAs or acidic peptides such as the C-terminal tail of tubulin (*37*)]. Our results show that the binding of heparin to K18ΔK280 and K18P301L is slightly weakened, and it is likely that this holds for other polyanions as well since our previous results showed that the same residues are important for microtubule and heparin binding (*25*). Despite the deletion of K280 in K18ΔK280, the NMR signals of V275−L284 were strongly influenced by the addition of heparin. On the other hand, signal intensities of residues S289−S293 appeared to be enhanced, and mutations affected only $^{1}H-^{15}N$ chemical shifts of residues in repeat 2 of the free protein. Therefore, we attribute the slightly reduced affinity for heparin to a combination of altered electrostatic properties and conformational changes.

The Interaction of the Repeat Domain of Tau with Microtubules Is More Specific than the Binding to Polyanions. Tau is a microtubule-associated protein that regulates diverse and essential MT functions, including polymerization and stabilization of MTs and modulation of MT dynamics (*14*). The domains flanking the repeat region bind strongly to MTs, even in the absence of the repeats, whereas the repeat motifs are essential for MT assembly (*48*). Notably, there are hot spots of MT binding, such as the KK motif (residues 280−281) in repeat R2 (*15*). FTDP-17-associated mutations, which cluster in the repeat region of tau, are known to weaken the interaction of tau with MTs and cause a decrease in the level of MT stabilization (*3*), whereas mutations which increase the concentration of 4Rtau lead to a decrease in the

dynamics of microtubules (*49*). Therefore, knowledge of the detailed mechanism by which the disease-associated mutations affect the ability of tau to bind to MTs is important. Here, we have characterized the binding of the repeat domain of tau, containing the two FTDP-17-linked mutations K18ΔK280 and K18P301L, to preassembled, paclitaxel-stabilized MTs on the level of individual residues.

Previously, we have shown that the binding of the repeat domain of tau to polyanions and paclitaxel-stabilized microtubules involves similar residues (*25*). K18 interacts with microtubules and heparin/poly-Glu through positive charges upstream of the PGGG motifs (K267-H268, H299, and H329) and through the hexapeptides at the beginning of repeats 2 and 3. In particular, I278 and K281 played an important role, in agreement with results obtained by site-directed mutagenesis (*15*). As poly-Glu resembles the Glu-rich C-terminal sequence of tubulin, the NMR data suggested that the positively charged clusters in the repeat domain bind to the C-terminus of tubulin. This is in agreement with biochemical studies showing an interaction between tau and the tubulin tail (*50*, *51*). The data presented here show that the binding of the two FTDP-17-linked mutations, K18ΔK280 and K18P301L, to microtubules differs from the binding to heparin. The disease-associated mutations reduce strongly the level of binding to MTs, whereas heparin binding is only slightly affected. In particular, the contribution of residues K274−L284 to MT binding is almost absent. This demonstrates that the binding to microtubules is more specific than a simple, electrostatically driven binding to polyanions. The directionality of changes in the $^{1}H-^{15}N$ chemical shifts induced by the mutations (see above) suggests that the detrimental effect of the mutations is due to an altered conformation centered around repeat 2 or a lack of an ability to form such a conformation upon binding, involving in particular the V275−K280 hexapeptide [note that the ΔK280 mutation strongly perturbs one of the MT-binding hot spots (*15*)]. Binding to heparin, on the other hand, does not require a specific conformational arrangement in the repeat domain of tau, or heparin can more easily adjust to a mutation-induced conformational change.

In interpreting the results reported here, one should recall that different modes of binding of tau to MT have been described in the literature. The predominant one, observed in most in vitro experiments and in cell-based experiments, shows tau as a molecule binding to the surface of microtubules rapidly and reversibly. At high tau:tubulin concentration ratios, this primary interaction can be complemented by a weak secondary interaction which has the hallmarks of unspecific "overloading" of the MT surface and can be avoided by increasing the ionic strength (see Figure 8; note that a high-salt step is typically included in the preparation of tubulin to eliminate MAPs). Another type of binding can occur when tau is copolymerized with tubulin; in this case, a fraction of tau appears to be trapped in the tubulin lattice in a fashion that is not readily reversible (*52*). This latter mode of binding does not apply here since the experiments were conducted with prepolymerized microtubules.

In summary, the two FTDP-17-associated mutations, ΔK280 and P301L, in the repeat domain of tau, which cause rapid aggregation in vitro, do not show significant changes in the secondary structure propensity of the soluble, monomeric protein. However, local structural changes in the second repeat are induced. The FTDP-17-associated mutations only slightly affect the binding to the polyanion heparin but significantly attenuate the binding to microtubules. This suggests that binding of four-repeat tau to microtubules involves specific interactions. Due to the reduced affinity of MT for four-repeat tau carrying the FTDP-17 mutations ΔK280 and P301L, more tau protein will be free in solution, increasing the effective concentration and thereby strengthening the tendency to aggregate. Aggregation nuclei formed by mutant tau could be elongated even from the pool of normal tau and thus poison the entire tau population in a cell.

ACKNOWLEDGMENT

We thank Sabrina Hübschmann for excellent technical help in protein preparation and Dr. Eva-Maria Mandelkow for stimulating discussions.

REFERENCES

1. D'Souza, I., Poorkaj, P., Hong, M., Nochlin, D., Lee, V. M., Bird, T. D., and Schellenberg, G. D. (1999) Missense and silent tau gene mutations cause frontotemporal dementia with parkinsonism-chromosome 17 type, by affecting multiple alternative RNA splicing regulatory elements, *Proc. Natl. Acad. Sci. U.S.A. 96*, 5598−5603.
2. Nacharaju, P., Lewis, J., Easson, C., Yen, S., Hackett, J., Hutton, M., and Yen, S. H. (1999) Accelerated filament formation from tau protein with specific FTDP-17 missense mutations, *FEBS Lett. 447*, 195−199.
3. von Bergen, M., Barghorn, S., Li, L., Marx, A., Biernat, J., Mandelkow, E. M., and Mandelkow, E. (2001) Mutations of tau protein in frontotemporal dementia promote aggregation of paired helical filaments by enhancing local β-structure, *J. Biol. Chem. 276*, 48165−48174.
4. Barghorn, S., Zheng-Fischhofer, Q., Ackmann, M., Biernat, J., von Bergen, M., Mandelkow, E. M., and Mandelkow, E. (2000) Structure, microtubule interactions, and paired helical filament aggregation by tau mutants of frontotemporal dementias, *Biochemistry 39*, 11714−11721.
5. Goedert, M., Jakes, R., Crowther, R. A., Hasegawa, M., Smith, M. J., and Spillantini, M. G. (1998) Intraneuronal filamentous tau protein and α-synuclein deposits in neurodegenerative diseases, *Biochem. Soc. Trans. 26*, 463−471.
6. Goedert, M., and Spillantini, M. G. (2000) Tau mutations in frontotemporal dementia FTDP-17 and their relevance for Alzheimer's disease, *Biochim. Biophys. Acta 1502*, 110−121.
7. Hutton, M., Lendon, C. L., Rizzu, P., Baker, M., Froelich, S., Houlden, H., Pickering-Brown, S., Chakraverty, S., Isaacs, A., Grover, A., Hackett, J., Adamson, J., Lincoln, S., Dickson, D., Davies, P., Petersen, R. C., Stevens, M., de Graaff, E., Wauters, E., van Baren, J., Hillebrand, M., Joosse, M., Kwon, J. M., Nowotny, P., Che, L. K., Norton, J., Morris, J. C., Reed, L. A., Trojanowski, J., Basun, H., Lannfelt, L., Neystat, M., Fahn, S., Dark, F., Tannenberg, T., Dodd, P. R., Hayward, N., Kwok, J. B., Schofield, P. R., Andreadis, A., Snowden, J., Craufurd, D., Neary, D., Owen, F., Oostra, B. A., Hardy, J., Goate, A., van Swieten, J., Mann, D., Lynch, T., and Heutink, P. (1998) Association of missense and 5′-splice-site mutations in tau with the inherited dementia FTDP-17, *Nature 393*, 702−705.
8. Goedert, M., Spillantini, M. G., Jakes, R., Rutherford, D., and Crowther, R. A. (1989) Multiple isoforms of human microtubule-associated protein tau: Sequences and localization in neurofibrillary tangles of Alzheimer's disease, *Neuron 3*, 519−526.
9. Buee, L., Laine, A., Delacourte, A., Flament, S., and Han, K. K. (1989) Qualitative and quantitative comparison of brain proteins in Alzheimer's disease, *Biol. Chem. Hoppe-Seyler 370*, 1229−1234.
10. Wischik, C. M., Novak, M., Edwards, P. C., Klug, A., Tichelaar, W., and Crowther, R. A. (1988) Structural characterization of the core of the paired helical filament of Alzheimer disease, *Proc. Natl. Acad. Sci. U.S.A. 85*, 4884−4888.
11. Wille, H., Drewes, G., Biernat, J., Mandelkow, E. M., and Mandelkow, E. (1992) Alzheimer-like paired helical filaments and

antiparallel dimers formed from microtubule-associated protein tau in vitro, *J. Cell Biol. 118*, 573−584.
12. Friedhoff, P., Schneider, A., Mandelkow, E. M., and Mandelkow, E. (1998) Rapid assembly of Alzheimer-like paired helical filaments from microtubule-associated protein tau monitored by fluorescence in solution, *Biochemistry 37*, 10223−10230.
13. von Bergen, M., Friedhoff, P., Biernat, J., Heberle, J., Mandelkow, E. M., and Mandelkow, E. (2000) Assembly of tau protein into Alzheimer paired helical filaments depends on a local sequence motif ((306)VQIVYK(311)) forming β structure, *Proc. Natl. Acad. Sci. U.S.A. 97*, 5129−5134.
14. Gustke, N., Trinczek, B., Biernat, J., Mandelkow, E. M., and Mandelkow, E. (1994) Domains of tau protein and interactions with microtubules, *Biochemistry 33*, 9511−9522.
15. Goode, B. L., and Feinstein, S. C. (1994) Identification of a novel microtubule binding and assembly domain in the developmentally regulated inter-repeat region of tau, *J. Cell Biol. 124*, 769−782.
16. Biernat, J., Gustke, N., Drewes, G., Mandelkow, E. M., and Mandelkow, E. (1993) Phosphorylation of Ser262 strongly reduces binding of tau to microtubules: Distinction between PHF-like immunoreactivity and microtubule binding, *Neuron 11*, 153−163.
17. Minoura, K., Yao, T. M., Tomoo, K., Sumida, M., Sasaki, M., Taniguchi, T., and Ishida, T. (2004) Different associational and conformational behaviors between the second and third repeat fragments in the tau microtubule-binding domain, *Eur. J. Biochem. 271*, 545−552.
18. DeTure, M., Ko, L. W., Yen, S., Nacharaju, P., Easson, C., Lewis, J., van Slegtenhorst, M., Hutton, M., and Yen, S. H. (2000) Missense tau mutations identified in FTDP-17 have a small effect on tau-microtubule interactions, *Brain Res. 853*, 5−14.
19. Schweers, O., Schonbrunn-Hanebeck, E., Marx, A., and Mandelkow, E. (1994) Structural studies of tau protein and Alzheimer paired helical filaments show no evidence for β-structure, *J. Biol. Chem. 269*, 24290−24297.
20. Goedert, M. (2005) Tau gene mutations and their effects, *Mov. Disord. 20* (Suppl. 12), S45−S52.
21. Bunker, J. M., Kamath, K., Wilson, L., Jordan, M. A., and Feinstein, S. C. (2006) FTDP-17 mutations compromise the ability of tau to regulate microtubule dynamics in cells, *J. Biol. Chem. 281*, 11856−11863.
22. Lu, M., and Kosik, K. S. (2001) Competition for microtubule-binding with dual expression of tau missense and splice isoforms, *Mol. Biol. Cell 12*, 171−184.
23. Ackmann, M., Wiech, H., and Mandelkow, E. (2000) Nonsaturable binding indicates clustering of tau on the microtubule surface in a paired helical filament-like conformation, *J. Biol. Chem. 275*, 30335−30343.
24. Avila, J., Lucas, J. J., Perez, M., and Hernandez, F. (2004) Role of tau protein in both physiological and pathological conditions, *Physiol. Rev. 84*, 361−384.
25. Mukrasch, M. D., Biernat, J., von Bergen, M., Griesinger, C., Mandelkow, E., and Zweckstetter, M. (2005) Sites of tau important for aggregation populate β-structure and bind to microtubules and polyanions, *J. Biol. Chem. 280*, 24978−24986.
26. Eliezer, D., Barre, P., Kobaslija, M., Chan, D., Li, X., and Heend, L. (2005) Residual structure in the repeat domain of tau: Echoes of microtubule binding and paired helical filament formation, *Biochemistry 44*, 1026−1036.
27. Wischik, C. M., Novak, M., Thogersen, H. C., Edwards, P. C., Runswick, M. J., Jakes, R., Walker, J. E., Milstein, C., Roth, M., and Klug, A. (1988) Isolation of a fragment of tau derived from the core of the paired helical filament of Alzheimer disease, *Proc. Natl. Acad. Sci. U.S.A. 85*, 4506−4510.
28. Delaglio, F., Grzesiek, S., Vuister, G. W., Zhu, G., Pfeifer, J., and Bax, A. (1995) NMRPipe: A multidimensional spectral processing system based on UNIX pipes, *J. Biomol. NMR 6*, 277−293.
29. Johnson, B. A., and Blevins, R. A. (1994) Nmr View: A Computer-Program for the Visualization and Analysis of Nmr Data, *J. Biomol. NMR 4*, 603−614.
30. Schwarzinger, S., Kroon, G. J., Foss, T. R., Wright, P. E., and Dyson, H. J. (2000) Random coil chemical shifts in acidic 8 M urea: Implementation of random coil shift data in NMRView, *J. Biomol. NMR 18*, 43−48.
31. Schwarzinger, S., Kroon, G. J., Foss, T. R., Chung, J., Wright, P. E., and Dyson, H. J. (2001) Sequence-dependent correction of random coil NMR chemical shifts, *J. Am. Chem. Soc. 123*, 2970−2978.
32. Wishart, D. S., and Sykes, B. D. (1994) Chemical shifts as a tool for structure determination, *Methods Enzymol. 239*, 363−392.
33. Wishart, D. S., Bigam, C. G., Holm, A., Hodges, R. S., and Sykes, B. D. (1995) ^{1}H, ^{13}C and ^{15}N random coil NMR chemical shifts of the common amino acids. I. Investigations of nearest-neighbor effects, *J. Biomol. NMR 5*, 67−81.
34. Lippens, G., Sillen, A., Smet, C., Wieruszeski, J. M., Leroy, A., Buee, L., and Landrieu, I. (2006) Studying the natively unfolded neuronal Tau protein by solution NMR spectroscopy, *Protein Pept. Lett. 13*, 235−246.
35. Dyson, H. J., and Wright, P. E. (2004) Unfolded proteins and protein folding studied by NMR, *Chem. Rev. 104*, 3607−3622.
36. Fasman, G. D. (1989) Protein conformational prediction, *Trends Biochem. Sci. 14*, 295−299.
37. Kampers, T., Friedhoff, P., Biernat, J., Mandelkow, E. M., and Mandelkow, E. (1996) RNA stimulates aggregation of microtubule-associated protein tau into Alzheimer-like paired helical filaments, *FEBS Lett. 399*, 344−349.
38. Goedert, M. (1996) Tau protein and the neurofibrillary pathology of Alzheimer's disease, *Ann. N.Y. Acad. Sci. 777*, 121−131.
39. Perez, M., Valpuesta, J. M., Medina, M., Montejo de Garcini, E., and Avila, J. (1996) Polymerization of tau into filaments in the presence of heparin: The minimal sequence required for tau-tau interaction, *J. Neurochem. 67*, 1183−1190.
40. Craik, D. J., and Wilce, J. A. (1997) Studies of protein-ligand interactions by NMR, *Methods Mol. Biol. 60*, 195−232.
41. Pawar, A. P., Dubay, K. F., Zurdo, J., Chiti, F., Vendruscolo, M., and Dobson, C. M. (2005) Prediction of "aggregation-prone" and "aggregation-susceptible" regions in proteins associated with neurodegenerative diseases, *J. Mol. Biol. 350*, 379−392.
42. Jicha, G. A., Rockwood, J. M., Berenfeld, B., Hutton, M., and Davies, P. (1999) Altered conformation of recombinant frontotemporal dementia-17 mutant tau proteins, *Neurosci. Lett. 260*, 153−156.
43. Barghorn, S., Davies, P., and Mandelkow, E. (2004) Tau paired helical filaments from Alzheimer's disease brain and assembled in vitro are based on β-structure in the core domain, *Biochemistry 43*, 1694−1703.
44. Cleveland, D. W., Kirschner, M. W., and Cowan, N. J. (1978) Isolation of separate mRNAs for α- and β-tubulin and characterization of the corresponding in vitro translation products, *Cell 15*, 1021−1031.
45. Goux, W. J. (2002) The conformations of filamentous and soluble tau associated with Alzheimer paired helical filaments, *Biochemistry 41*, 13798−13806.
46. Sadqi, M., Hernandez, F., Pan, U., Perez, M., Schaeberle, M. D., Avila, J., and Munoz, V. (2002) α-Helix structure in Alzheimer's disease aggregates of tau-protein, *Biochemistry 41*, 7150−7155.
47. Berriman, J., Serpell, L. C., Oberg, K. A., Fink, A. L., Goedert, M., and Crowther, R. A. (2003) Tau filaments from human brain and from in vitro assembly of recombinant protein show cross-beta structure, *Proc. Natl. Acad. Sci. U.S.A. 100*, 9034−9038.
48. Preuss, U., Biernat, J., Mandelkow, E. M., and Mandelkow, E. (1997) The 'jaws' model of tau-microtubule interaction examined in CHO cell, *J. Cell Sci. 110*, 789−800.
49. Bunker, J. M., Wilson, L., Jordan, M. A., and Feinstein, S. C. (2004) Modulation of microtubule dynamics by tau in living cells: Implications for development and neurodegeneration, *Mol. Biol. Cell 15*, 2720−2728.
50. Littauer, U. Z., Giveon, D., Thierauf, M., Ginzburg, I., and Ponstingl, H. (1986) Common and distinct tubulin binding sites for microtubule-associated proteins, *Proc. Natl. Acad. Sci. U.S.A. 83*, 7162−7166.
51. Serrano, L., Montejo de Garcini, E., Hernandez, M. A., and Avila, J. (1985) Localization of the tubulin binding site for tau protein, *Eur. J. Biochem. 153*, 595−600.
52. Makrides, V., Massie, M. R., Feinstein, S. C., and Lew, J. (2004) Evidence for two distinct binding sites for tau on microtubules, *Proc. Natl. Acad. Sci. U.S.A. 101*, 6746−6751.

BI061318S